Vibrationally resolved photofragment spectroscopy of FeO^+

John Husband, Fernando Aguirre, Peter Ferguson, and Ricardo B. Metz
Department of Chemistry, University of Massachusetts-Amherst, Amherst, Massachusetts 01003

(Received 11 February 1999; accepted 26 April 1999)

We report the first vibrationally resolved spectroscopic study of FeO^+. We observe the $0\leftarrow0$ and $1\leftarrow0$ bands of a $^6\Sigma\leftarrow X\,^6\Sigma$ transition at 28 648.7 and 29 311 cm^{-1}. Under slightly modified source conditions the $1\leftarrow1$ transition is observed at 28 473 cm^{-1}. In addition to establishing an *upper limit* $D_0^o(Fe^+-O)\leqslant342.7$ kJ/mol, our results give the first experimental measurements of the vibrational frequencies in both the ground state, $\nu_0''=838\pm4$ cm^{-1}, and the excited electronic state, $\nu_0'=662\pm2$ cm^{-1}. Partially resolved rotational structure underlying the vibrational peaks has been analyzed to measure the predissociation lifetime and estimate the change in molecular constants upon electronic excitation. © *1999 American Institute of Physics.* [S0021-9606(99)00328-1]

I. INTRODUCTION

The chemistry of gas-phase transition metal oxide cations (MO^+) has received a great deal of attention, primarily due to their ability to selectively oxidize a variety of organic molecules.[1] Much of this interest has centered on FeO^+ because of its ability to activate methane under thermal conditions:[2,3]

$$FeO^+ + CH_4 \rightarrow Fe^+ + CH_3OH. \quad (1)$$

The reactions of FeO^+ with H_2 and CH_4 have been studied in detail in the laboratories of Schwarz, Armentrout, and Bohme; a recent paper summarizes the results of all three groups, which span a broad range of pressures and experimental conditions.[4] FeO^+ reacts inefficiently with H_2, but reacts with moderate efficiently with methane ($k=7.4\pm2.2\times10^{-11}\,cm^3\,s^{-1}$ under thermal conditions), producing $Fe^+ + CH_3OH$ (39%) and $FeOH^+ + CH_3$ (61%) as the major products.[4] The Fe^+-O bond strength was measured via bracketing reactions by Kappes and Staley in 1981,[5] and by Beauchamp and co-workers[6] in 1982 using a guided ion beam spectrometer. The most reliable values are based on recent studies of the endothermic reactions of Fe^+ with O_2 and ethylene oxide in a second-generation guided ion beam spectrometer.[7] Armentrout has recently reevaluated[8] these results to determine $D_0^o(Fe^+-O)=335\pm5$ kJ/mol. In the only spectroscopic investigation of FeO^+ to date Freiser and coworkers measured the photofragment spectrum of FeO^+, observing a gradual onset at ~420 nm leading to a sharp feature near 350 nm whose width was determined by the ~10 nm resolution of their spectrometer.[9] From the dissociation onset they assigned $D^o(Fe^+-O)=285\pm20$ kJ/mol.

FeO^+ (Refs. 10–14) and its reactions with H_2 (Refs. 15–17) and CH_4 (Ref. 18) have been the subject of many *ab initio* studies. Fiedler *et al.* used density functional theory and the complete active space perturbation theory CASPT2D to study the ground and low-lying excited electronic states of late first-row transition metal oxides.[19] They predict that FeO^+ has a $^6\Sigma$ ground state and three low-lying quartet states at energies of 1.0 to 1.4 eV. Higher-lying states were not calculated. In a separate study[14] Fielder *et al.* used multireference perturbation theory to calculate the spectroscopic constants of FeO^+, predicting $r_e=1.643$ Å, $\omega_e=915.2$ cm^{-1} ($\nu_0=915.7\,cm^{-1}$) and $D^o=338.9$ kJ/mol, in good agreement with the measured value.[8] Recent *ab initio* calculations suggest that the mechanism for methane activation by the enzyme soluble methane monooxygenase is similar to that of gas-phase FeO^+. FeO^+ has therefore been proposed as a model for the active site in the enzyme.[20]

FeO^+ is important in the iron chemistry of the mesosphere[21] and has been detected mass-spectrometrically at altitudes near 90 km where it is produced by the reaction of Fe^+ (introduced by meteorites) with ozone.[22] In addition, Kopp *et al.* used the known rates of the $Fe^+ + O_3$ and $FeO^+ + O$ reactions to estimate mesospheric [O] from their measured $[Fe^+]$ and $[FeO^+]$ and satellite measurements of $[O_3]$.[22]

As part of an effort to spectroscopically characterize the reactants and intermediates[3] of the $FeO^+ + CH_4$ reaction we report the first vibrationally resolved spectroscopic study of gas-phase FeO^+.

II. EXPERIMENTAL APPROACH

The experiment involves the photodissociation of ions in the dual time-of-flight mass spectrometer shown in Fig. 1. Briefly, ions produced in the source are mass selected, photodissociated at the turning point of a reflectron, and the masses of fragment ions determined by time-of-flight.

FeO^+ ions are produced in a standard laser ablation source.[23,24] The frequency-doubled output of a pulsed Nd:YAG laser (Continuum Surelite I, **1** in Fig. 1) operating at 20 Hz repetition rate is loosely focused onto a rotating and translating iron rod (**2**) (Sigma-Aldrich, 99.98% pure). The resulting plasma is entrained in a pulse of gas (**3**) introduced through a home-built piezoelectric pulsed valve.[25] Fe^+ ions produced by ablation react with N_2O (Merriam–Graves, 99.8% pure) in the gas pulse to produce FeO^+,[26] which expands through a 2.5 mm dia., 4.5 mm long tube into the source vacuum chamber. After 10 cm the beam is skimmed and ions pass into the differential chamber. The source chamber is maintained below 5×10^{-5} Torr by a 2400 ℓ/s

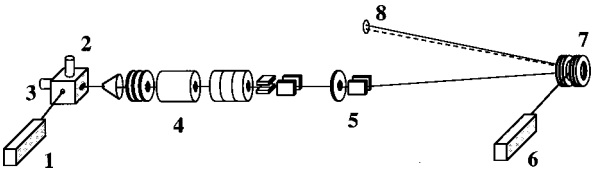

FIG. 1. Schematic view of the photofragment spectrometer. Labels are described in the text.

diffusion pump (Varian VHS-6) and the differential chamber is kept below 3×10^{-6} Torr by a baffled diffusion pump (Varian VHS-4, 600 ℓ/s throughput). The apparatus can be run as either a beam-modulated time-of-flight mass spectrometer[27,28] or in a coaxial Wiley–McLaren configuration.[29] Signal levels are typically a factor of five larger in the Wiley–McLaren configuration, which was used for these studies. Ions are extracted along the beam axis using a pulsed electric field, then accelerated to 1800 V kinetic energy. It is convenient to have the source and flight tube grounded, so, after acceleration, the ions must be rereferenced to ground potential.[30] This is accomplished by maintaining the rereferencing tube (**4**) at −1800 V as the ion cloud enters, then rapidly pulsing it to ground prior to the ions' exit using a potential switch.[31] An Einzel lens and deflectors guide the ions through an aperture into the detector chamber, which is maintained below 2×10^{-7} Torr by a 240 ℓ/s ion pump (Varian VacIon Plus 300 StarCell). A final deflector (**5**) allows the ion beam to traverse the 5° angle through the reflectron and onto the detector. When the deflector is off, <0.1% of the incident ions reach the detector. Applying a pulsed voltage to the deflector allows only ions within a few mass units of the ion of interest to reach the detector, forming an effective mass gate. This is very valuable in the present studies as, without the mass gate, the large peak from Fe^+, which is by far the most abundant ion, affects the baseline in the rest of the mass spectrum.

The unfocused output of a frequency-doubled pulsed, tunable dye laser (**6**) (Continuum ND6000, Continuum Powerlite 8020 pump), linewidth <0.2 cm^{-1} near 350 nm, interacts with the mass-selected ion at the turning point[32] of the reflectron[33,34] (**7**) and the masses of charged dissociation fragments (dashed lines in the figure) are determined by their subsequent flight times to a 40 mm dia. dual microchannel plate detector (**8**) (Galileo Electro-optics). The resulting signal is amplified tenfold by a high-speed amplifier and collected on a 500 MHz digital oscilloscope (Tektronics 524A). Parent ion resolution at the turning point of the reflectron is $m/\Delta m\approx150$ while that for the photofragments at the detector is $m/\Delta m\approx100$. Photodissociation pathways and branching ratios are obtained from the difference between mass spectra collected with the photodissociation laser blocked and unblocked. In these studies Fe^+ is the only fragment ion observed, as expected. The photofragment spectrum is obtained by monitoring the yield of a specific fragment ion as a function of laser wavelength and normalizing to parent ion signal and laser power. A LabView-based program running on a PowerMacintosh computer reads the digitized output of fast gated integrators (Stanford Research Systems SR250) monitoring parent and fragment ion signals.

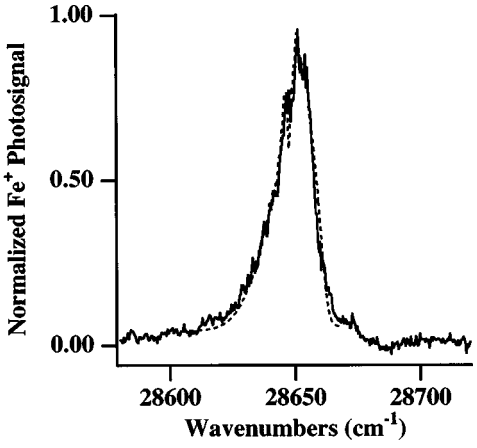

FIG. 2. Photofragment spectrum of $^{56}FeO^+$, showing the 0←0 transition (solid lines) and best-fit simulation (dashed lines).

Various gas mixtures and backing pressures are used to minimize production of vibrationally excited ions. Best results are achieved with 3% N_2O and 15% N_2 in He at a backing pressure of 4 atm. Dissociation is linear with laser fluences up to ~1 mJ/cm^2 for the 0←0 transition, and >10 mJ/cm^2 for the 1←0 transition. The laser wavelength is calibrated using the photoacoustic vibrational overtone spectrum of H_2O near 700 nm.[35] Our reported spectra include a 0.25 cm^{-1} Doppler shift due to the transverse ion beam velocity at the turning point of the reflectron.

III. RESULTS

The photofragment spectrum of internally cold FeO^+ shows two clear peaks in the region 27 600–32 400 cm^{-1}. The intense peak near 28 650 cm^{-1} is shown in Fig. 2; the much weaker feature near 29 310 cm^{-1} is in Fig. 3. The peaks are asymmetric and have widths of 15 and 40 cm^{-1}, respectively. We also observe a 400 cm^{-1}-wide feature near 30 500 cm^{-1} which is an order-of-magnitude less intense than that at 29 310 cm^{-1}. Extremely low levels of background nonresonant signal are found throughout the range covered. When helium alone is used as a bath gas, FeO^+ is

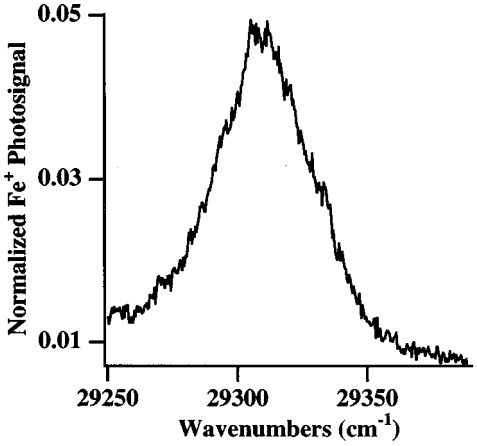

FIG. 3. Photofragment spectrum of the 1←0 transition in $^{56}FeO^+$. The intensity scale is relative to the 0←0 band.

less efficiently cooled and an additional band is observed near 28 470 cm^{-1}. Less efficient cooling also leads to a more pronounced asymmetry in the observed peaks, as well as a general increase in the nonresonant signal level.

Freiser and co-workers[9] obtained the photofragment spectrum of FeO^+ in an ion cyclotron resonance spectrometer using a lamp–monochromator combination with 10 nm (800 cm^{-1} at 350 nm) resolution, observing a peak near 350 nm whose low-intensity tail extends to 420 nm. The width of the peak is determined by the resolution of their spectrometer. The apparent threshold at 420 nm was used to assign $D^o(Fe^+–O)=285\pm20$ kJ/mol. The peak shown in Fig. 2 clearly corresponds to the feature they observe at 350 nm (28 600 cm^{-1}). Our study suggests their observed tailing to low energy is due to internally excited ions, giving rise to an anomalously low threshold. Our results are indicative of transitions to a predissociative state, with a lifetime sufficient to observe vibrational structure. The observed peaks correspond to 0←0 and 1←0 transitions, at 28 648.7 and 29 311 cm^{-1}, respectively, and a 1←1 transition at 28 473 cm^{-1}. Peak positions are based on rotational simulations (see below). The energy of the 0←0 transition establishes the *upper limit* $D_0^o(Fe^+–O)\leqslant342.7$ kJ/mol. This value is consistent with the thermodynamic value for $D_0^o(Fe^+–O)$ of 335 ± 5 kJ/mol reported by Armentrout and co-workers[7,8] based on the endothermic $Fe^+ + O_2$ reaction. Since dissociation of FeO^+ $(X\,^6\Sigma)$ to electronically excited $Fe^+(^4F_0)+O(^3P_0)$ requires 357 ± 5 kJ/mol,[36] we must observe dissociation to ground electronic state fragments $Fe^+(^6D_J)+O(^3P_J)$.

The positions of the three peaks allow the first experimental determination of the vibrational frequencies in both the ground $(X\,^6\Sigma^+)$ state, $(\nu_0''=838\pm4\ cm^{-1})$ and the predissociative state $(\nu_0'=662\pm2\ cm^{-1})$. A Franck–Condon analysis of the integrated intensities of the 0←0 and 1←0 transitions (10:1) allows an estimation of the change in Fe^+–O bond length upon excitation of 0.024 ± 0.004 Å. Fielder *et al.* predict $\nu_0''=915.7\ cm^{-1}$ using multireference perturbation theory, in good agreement with our measured value considering the difficulty of calculations on high spin systems.[14] The vibrational frequency of FeO^+ is surprisingly close to the 832.41 cm^{-1} value measured for the isoelectronic MnO $(X\,^6\Sigma^+)$ radical.[37]

In addition to the vibrational structure discussed above, the spectrum also contains rotational information. While the resolution is insufficient to show discrete rotational lines, reproducible features are observed. The 0←0 band is shown in Fig. 2 with a simulation of the underlying rotational envelope. Concentrating initially on the observed band we see partially resolved rotational structure: a single intense peak that tails to low energy. *Ab initio* calculations indicate a $^6\Sigma$ ground state for FeO^+.[14] Observation of a single intense peak for the 0←0 band points to the predissociative state also being a $^6\Sigma$ state. The tailing to low energies is characteristic of a lengthening of the FeO^+ bond upon excitation.

The rotational structure in the 0←0 band was simulated assuming a $^6\Sigma\leftarrow{}^6\Sigma$ transition. The large spin–spin interactions found in systems containing transition metals often make these systems intermediate between Hund's cases (a) and (b) for low lying rotational levels. The standard Hamiltonian[37]

$$\mathcal{H}=B(\mathbf{J}-\mathbf{S})^2-D(\mathbf{J}-\mathbf{S})^4+\gamma(\mathbf{J}-\mathbf{S})\mathbf{S}+\tfrac{2}{3}\lambda(3Sz^2-\mathbf{S}^2), \tag{2}$$

for a $^6\Sigma$ state was diagonalized in a Hund's case (a) basis, and transition intensities obtained following the procedures outlined by Hougen.[38] To account for lifetime broadening, the resulting spectrum was convoluted with a Lorentzian of appropriate width.[39]

TABLE I. Molecular constants for $^{56}FeO^+$ (calculated) and ^{55}MnO (experimental).

Constant	$^{56}FeO^+$ $(X\,^6\Sigma^+)$	^{55}MnO $(X\,^6\Sigma^+)$
r_0 (Å) (B_0 (cm^{-1}))	1.648 [a] (0.4991) [a]	1.647 [b] (0.501 21) [b]
ν_0 (cm^{-1})	915.7 [a]	832.41 [c]
D_0 (cm^{-1})	5.793×10^{-7} [a]	7.190×10^{-7} [b]
λ (cm^{-1})		0.574 [b]
γ (cm^{-1})		−0.0024 [b]

[a]Reference 14. Equilibrium values have been converted to $v=0$ values.
[b]Reference 40.
[c]Reference 37.

Although the observed band contour is sufficient to yield some rotational information, discrete rotational lines are required before full assignment of all molecular constants can be made. In the absence of such lines it is necessary to constrain the simulation parameters somewhat. One means to this end involves fixing the ground state constants and optimizing the upper state constants; in effect estimating the differences in molecular constants for the upper and ground states rather than their absolute values. A requirement of this method is a good approximation of the ground state constants. The results of the calculations performed by Fielder *et al.*[14] for FeO^+ $(X\,^6\Sigma)$ are summarized in Table I. Unfortunately, the complete set of ground state molecular constants needed for our rotational simulation were not calculated. The MnO $(X\,^6\Sigma)$ radical, isoelectronic with FeO^+, has been the subject of several high-resolution spectroscopic studies.[37,40,41] Molecular constants for MnO are also shown in Table I. The strong similarities between the calculated values for FeO^+ and the experimentally determined values for MnO suggest that MnO is a good model for FeO^+. For consistency we use only MnO values for the ground state rather than a mixture of MnO and calculated FeO^+ values. Although Merer and co-workers observe a $^6\Sigma\leftarrow{}^6\Sigma$ transition in MnO,[37,41] this transition is centered near 550 nm (18 000 cm^{-1}), and therefore does not correspond to the transition observed in our study.

A further reduction of simulation parameters can be made. The MnO $(X\,^6\Sigma)$ values for the centrifugal distortion constant D, and the spin–rotational coupling constant γ, are 7.190×10^{-7} and $-0.0024\ cm^{-1}$, respectively. In the present study the experimental resolution, limited by the lifetime in the predissociative state, is 1.5 cm^{-1}. At this resolution, and at the low rotational levels populated in a molecular beam, contributions from D and γ are not significant. They were consequently set to zero in the simulations, reducing the

TABLE II. Optimized molecular constants for $^{56}FeO^+$.

Constant	$X^6\Sigma$ ($v''=0$)	Upper $^6\Sigma(v'=0)$	Upper $^6\Sigma(v'=1)$
T_0 (cm^{-1})	0	28 648.7±0.1	29311±2
r (Å)	1.647 [a]	1.674±0.005	
B (cm^{-1}) [b]	0.501 21 [a]	0.484±0.003	
λ (cm^{-1})	0.574 [a]	0.7±0.1	
τ (ps)		3.5	0.14

[a]Values correspond to MnO constants (Ref. 40) and were not optimized in the present study. See text.
[b]B values for corresponding r values. Shown for reference.

number of free parameters to five: the term value T_0, bond length r', spin–spin coupling constant λ', the excited state lifetime τ, and the rotational temperature. These parameters were optimized in a nonlinear least-squares routine[42] to obtain the fit shown with dashed lines in Fig. 2. It was found that a mixture of two rotational temperatures is required to match the observed band shape. For the spectrum shown in Fig. 2 the best fit was achieved with 80% of the molecules at a rotational temperature of 8 K and the remainder at 72 K. Resulting, best-fit molecular parameters are summarized in Table II.

The rotational simulations predict a change in bond length $\Delta r = 0.027 \pm 0.005$ Å for the 0←0 transition, consistent with the $\Delta r = 0.024 \pm 0.004$ Å predicted from the Franck–Condon overlap. This relatively small change in bond length is consistent with an excitation between molecular orbitals centered on iron rather than a charge transfer transition from the oxygen atom to the iron.[43] The values of the spin–spin coupling constants used for the simulation shown in Fig. 2 are $\lambda''=0.574$ cm^{-1} and $\lambda'=0.7\pm0.1$ cm^{-1}. These are effective coupling constants with contributions from direct spin–spin coupling and second-order spin–orbit coupling $\lambda_{eff}=\lambda^{SS}+\lambda^{SO}$. For a molecule such as FeO^+ containing heavy atoms the largest contribution to λ_{eff} would be expected to come from the second-order spin–orbit coupling.[39] A series of simulations was performed using larger values of λ', in an attempt to interpret the three peaks in the 0←0 band as spin structure and deemphasize the need for two rotational temperatures. These simulations lead to spectra with a pronounced central dip and fail to capture the observed width.

The 1←0 peak is much broader than the 0←0 transition. The rotational simulations suggest a linewidth of 39 cm^{-1}, corresponding to a lifetime in the $v'=1$ state of 0.14 ps. The quality of the fit is unaffected by any physically reasonable value of r' or λ'.

In conclusion we report the first vibrationally resolved spectroscopic study of FeO^+. We observe the 0←0 and 1←0 bands of a $^6\Sigma \leftarrow X\,^6\Sigma$ transition. Under slightly modified source conditions the 1←1 transition is observed. In addition to supporting thermodynamic information given by ion beam experiments by Armentrout and co-workers,[7,8] our results give the first experimental measurements of the vibrational frequencies in both the ground and an excited electronic state. Partially resolved rotational structure underlying the vibrational peaks has been analyzed to estimate the differences in molecular constants between the ground and upper states.

ACKNOWLEDGMENT

We gratefully acknowledge the support of this work by a Camille and Henry Dreyfus New Faculty Award.

[1] D. Schröder and H. Schwarz, Angew. Chem. Int. Ed. Engl. **34**, 1973 (1995).
[2] D. Schröder and H. Schwarz, Angew. Chem. Int. Ed. Engl. **29**, 1433 (1990).
[3] D. Schröder, A. Fiedler, J. Hrusák, and H. Schwarz, J. Am. Chem. Soc. **114**, 1215 (1992).
[4] D. Schröder, H. Schwarz, D. E. Clemmer, Y. Chen, P. B. Armentrout, V. Baranov, and D. K. Bohme, Int. J. Mass Spectrom. Ion Processes **161**, 175 (1997).
[5] M. M. Kappes and R. H. Staley, J. Phys. Chem. **85**, 942 (1981).
[6] P. B. Armentrout, L. F. Halle, and J. L. Beauchamp, J. Chem. Phys. **76**, 2449 (1982).
[7] S. K. Loh, E. R. Fisher, L. Lian, R. H. Schultz, and P. B. Armentrout, J. Phys. Chem. **93**, 3159 (1989).
[8] P. B. Armentrout and B. L. Kickel, in *Organometallic Ion Chemistry*, edited by B. S. Freiser (Kluwer Academic, Dordrecht, The Netherlands, 1994).
[9] R. L. Hettich, T. C. Jackson, E. M. Stanko, and B. S. Freiser, J. Am. Chem. Soc. **108**, 5086 (1986).
[10] M. Krauss and W. J. Stevens, J. Chem. Phys. **82**, 5584 (1985).
[11] E. A. Carter and W. A. Goddard, J. Phys. Chem. **92**, 2109 (1988).
[12] M. N. Glukhovtsev, R. D. Bach, and C. J. Nagel, J. Phys. Chem. A **101**, 316 (1997).
[13] E. G. Bakalbassis, M.-A. D. Stiakaki, A. C. Tsipis, and C. A. Tsipis, Chem. Phys. **223**, 169 (1997).
[14] A. Fiedler, J. Hrusák, W. Koch, and H. Schwarz, Chem. Phys. Lett. **211**, 242 (1993).
[15] D. Schröder, A. Fiedler, M. Ryan, and H. Schwarz, J. Phys. Chem. **98**, 68 (1994).
[16] D. Danovich and S. Shaik, J. Am. Chem. Soc. **119**, 1773 (1997).
[17] M. Filatov and S. Shaik, J. Phys. Chem. A **102**, 3835 (1998).
[18] K. Yoshizawa, Y. Shiota, and T. Yamabe, J. Am. Chem. Soc. **120**, 564 (1998).
[19] A. Fiedler, D. Schröder, S. Shaik, and H. Schwarz, J. Am. Chem. Soc. **116**, 10734 (1994).
[20] K. Yoshizawa, J. Biol. Inorg. Chem. **3**, 318 (1998).
[21] T. J. Kane and C. S. Gardner, J. Geophys. Res. **98**, 16875 (1993).
[22] E. Kopp, P. Eberhardt, U. Herrmann, and L. G. Bjoern, J. Geophys. Res. **90**, 13041 (1985).
[23] T. G. Dietz, M. A. Duncan, D. E. Powers, and R. E. Smalley, J. Chem. Phys. **74**, 6511 (1981).
[24] P. J. Brucat, L.-S. Zheng, C. L. Pettiette, S. Yang, and R. E. Smalley, J. Chem. Phys. **84**, 3078 (1986).
[25] D. Proch and T. Trickl, Rev. Sci. Instrum. **60**, 713 (1989).
[26] R. L. Hettich and B. S. Freiser, J. Am. Chem. Soc. **108**, 2537 (1986).
[27] J. M. B. Bakker, J. Phys. E **6**, 785 (1973).
[28] J. M. B. Bakker, J. Phys. E **7**, 364 (1974).
[29] W. C. Wiley and I. H. McLaren, Rev. Sci. Instrum. **26**, 1150 (1955).
[30] L. A. Posey, M. J. DeLuca, and M. A. Johnson, Chem. Phys. Lett. **131**, 170 (1986).
[31] R. E. Continetti, D. R. Cyr, and D. M. Neumark, Rev. Sci. Instrum. **63**, 1840 (1992).
[32] D. S. Cornett, M. Peschke, K. Laitting, P. Y. Cheng, K. F. Willey, and M. A. Duncan, Rev. Sci. Instrum. **63**, 2177 (1992).
[33] V. I. Karataev, B. A. Mamyrin, and D. V. Shmikk, Sov. Phys. Tech. Phys. **16**, 1177 (1972).
[34] B. A. Mamyrin, V. I. Karataev, D. V. Shmikk, and V. A. Zagulin, Sov. Phys. JETP **37**, 45 (1973).
[35] L. S. Rothman, R. R. Gamache, A. Goldman, L. R. Brown, R. A. Toth, H. M. Pickett, R. L. Poynter, J.-M. Flaud, C. Camy-Peyret, A. Barbe, N. Husson, C. P. Rinsland, and M. A. H. Smith, Appl. Opt. **26**, 4058 (1987).
[36] C. E. Moore, NBS Circ. No. 467 (U.S. Dept. of Commerce, Washington, D.C., 1952), Vol. II.
[37] R. M. Gordon and A. J. Merer, Can. J. Phys. **58**, 642 (1980).

[38] J. T. Hougen, *The Calculation of Rotational Energy Levels and Rotational Intensities in Diatomic Molecules*, National Bureau of Standards Monograph 115, Washington, D.C., 1970.
[39] H. Lefebvre-Brion and R. Field, *Perturbations in the Spectra of Diatomic Molecules* (Academic, London, 1986).
[40] K. Namiki and S. Saito, J. Chem. Phys. **107**, 8848 (1997).
[41] A. G. Adam, Y. Azuma, H. Li, A. J. Merer, and T. Chandrakumar, Chem. Phys. **152**, 391 (1991).
[42] W. H. Press, S. A. Teukolsky, W. T. Vetterling, and B. P. Flannery, *Numerical Recipies in C: The Art of Scientific Computing*, 2nd ed. (Cambridge University, New York, 1992).
[43] A. J. Merer, Annu. Rev. Phys. Chem. **40**, 407 (1989).